

Tunneling spectroscopy of $R\text{Te}_2$ ($R=\text{La}, \text{Ce}$) and possible coexistence between charge-density waves and magnetic order

M. H. Jung*

Department of Quantum Matter, ADSM, Hiroshima University, Higashi-Hiroshima 739-8526, Japan

T. Ekino

Faculty of Integrated Arts and Sciences, Hiroshima University, Higashi-Hiroshima 739-8521, Japan

Y. S. Kwon

Department of Physics, Sung Kyun Kwan University, Suwon 440-746, South Korea

T. Takabatake

Department of Quantum Matter, ADSM, Hiroshima University, Higashi-Hiroshima 739-8526, Japan

(Received 5 September 2000; published 22 December 2000)

Tunneling spectra are measured on the charge-density wave (CDW) compound LaTe_2 and the isostructural antiferromagnet CeTe_2 with $T_N=4.3$ K by a break-junction method. In contrast to the well-developed CDW gap $2\Delta=0.9$ eV wide for LaTe_2 , the spectrum of polycrystal CeTe_2 is V shaped with $2\Delta=1.2$ eV. These gap structures agree with the optical-conductivity spectra for both compounds. The V-shaped spectrum for CeTe_2 suggests that the CDW gap is modified by the presence of electronic states hybridized with the $4f$ electron states. A smaller gap $2\Delta^*=0.5$ eV was observed for the bulk tunneling current in the c plane of single crystals of CeTe_2 . On cooling below $T_C=6.1$ K, where a short-range ferromagnetic order sets in, $2\Delta^*$ exhibits a sharp minimum. Furthermore, subgap anomalies appear below T_C and suddenly increase at T_N . The normalized zero-bias conductance shows a minimum at T_C and a sudden increase below T_N . These facts suggest possible interplay of CDW's and magnetic order in CeTe_2 .

DOI: 10.1103/PhysRevB.63.035101

PACS number(s): 71.45.Lr, 71.20.Eh, 73.40.Gk, 75.50.Ee

Charge-density waves (CDW's) occur in numbers of low-dimensional materials, of which the electronic instabilities lead to their structural modulations.¹ The CDW instability driven by Fermi surface nesting has a tendency to lower the electronic energy by opening an energy gap at the Fermi level. Electron-tunneling spectroscopy provides direct observation of the energy gap because the tunneling conductance is proportional to the electronic density of states.² The competition between CDW condensation and superconductivity was found in certain systems.³ The coexistence between CDW's and magnetic order has recently been reported for a rare-earth based compound $\text{Er}_5\text{Ir}_4\text{Si}_{10}$.⁴ To the best of our knowledge, however, no evidence for the interplay of CDW's with magnetism has been reported yet.

Layered compounds such as transition-metal dicalcogenides TX_2 (T =transition metal; X =S, Se, Te)⁵ and rare-earth polychalcogenides RX_n (R =rare earth; $n=2,2.5,3$)⁶⁻¹⁰ are susceptible to the CDW formation due to the electronic instability. The compounds RX_2 with the layered tetragonal Cu_2Sb -type structure¹¹ consist of rare-earth-chalcogen layers separated by a chalcogen square sheet. Commensurate CDW was observed in $\text{RSe}_{1.9}$ ($R=\text{La}, \text{Ce}, \text{Pr}$), where Se dimmers and ordered vacancies lead to distorted Se sheet superstructure.⁶ On the other hand, incommensurate CDW in SmTe_3 was reported to be stable at room temperature.⁹ The strong anisotropy in the gap of $2\Delta\approx 0.5$ eV was revealed by the angle-resolved photoemission spectroscopy.¹⁰

For LaTe_2 , a periodic lattice distortion was observed through transmission electron microscopy.¹² It was shown that the CDW's with the superlattice wave vector $q=a^*/2$

are stable even at room temperature. Band calculations of LaTe_2 suggested that the CDW states arise from the nesting between the electron and hole Fermi surfaces of the Te square sheet.^{12,13} However, no direct evidence of the CDW gap in LaTe_2 has been given to date. Recently, we have grown high-quality single-crystalline samples of $\text{CeTe}_{2-\delta}$ ($\delta\approx 0.15$).¹⁴ This value of δ is common to $\text{SmTe}_{1.84}$ and $\text{DySe}_{1.85}$, which was ascribed to the defective Te layers buildup isolated Te.^{6,7,9,15} This vacancy stabilizes the dimerization of Te ions and the structural modulation,^{15,16} resulting in semiconducting behavior of the electrical resistivity.^{14,17} The electronic band structure of CeTe_2 is in nature analogous to that of LaTe_2 except the existence of the $4f$ state, which is believed to deform the gap because of the hybridization between the Ce $4f$ state and the Te $5p$ hole band in the Te sheet.^{14,18} Recently, the possible presence of CDW's has been suggested in CeTe_2 from the electrical resistivity measurements.^{14,18} The c -axis resistivity $\rho_{\parallel c}$ exhibits a semiconducting temperature dependence of the order of a few tens of Ω cm, while the c -plane resistivity $\rho_{\perp c}$ shows a broad maximum at 100 K and then decreases on cooling, resulting in the resistivity ratio $\rho_{\parallel c}/\rho_{\perp c}\sim 150$ at 1.5 K.¹⁴ At low temperatures, CeTe_2 undergoes two characteristic transitions. The electrical resistivity exhibits a sharp peak at $T_C=6.1$ K,^{14,18} below which a two-dimensional ferromagnetic order develops in the CeTe layer. Below $T_N=4.3$ K, a three-dimensional antiferromagnetic order occurs among the ferromagnetic CeTe layers in the spin sequence up-down-down-up along the c axis.^{19,20} It should be interesting if the magnetic orders in CeTe_2 have significant effect on the CDW gap.

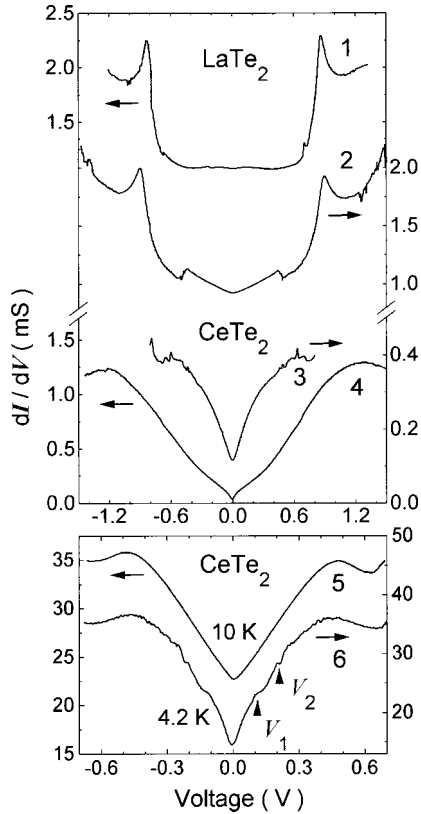


FIG. 1. Differential tunneling conductance dI/dV for polycrystalline samples of LaTe_2 and CeTe_2 . Top: the typical dI/dV curve measured at 60 K (curve 1) for LaTe_2 dI/dV for LaTe_2 at 30 K (curve 2) exhibits double-gap structures due to SIN and SIS junctions. The spectra for CeTe_2 at 77 K (curve 3) and 55 K (curve 4) correspond to SIN and SIS junctions, respectively. Bottom: dI/dV for a junction of CeTe_2 at 4.2 K (curve 6) and 10 K (curve 5). The arrows indicate subgap anomalies.

In this paper, we report electron-tunneling experiments on LaTe_2 and CeTe_2 . The results give the evidence for the CDW gap in these compounds. We have used an *in situ* break-junction method, which prevents Ce-based compounds from serious surface oxidation.²¹ A platelet sample with its cross section $\sim 0.1 \times 2 \text{ mm}^2$ was mounted on a flexible substrate and cracked at 4.2 K by applying an adjustable bending force. In this way, we were able to make stable tunneling junctions with a clean interface. The tunneling conductance dI/dV was measured by an ac-modulation technique with a four-probe method. If a few junctions coexist at the interface, then the observed conductance is a superposition of contributions from each junction, where the tunneling current may strongly depend on the surface state and geometry with respect to the crystallographic axis.²¹ In order to study the possible interplay between the magnetic order and CDW in CeTe_2 , we have measured the temperature and magnetic-field dependence of the tunneling spectra in the vicinity of T_C and T_N , using single-crystalline samples. We confirmed that the stoichiometry, electrical resistivity, and magnetic susceptibility of the present samples agree with previous results.¹⁴

Figure 1 shows representative data of dI/dV for polycrys-

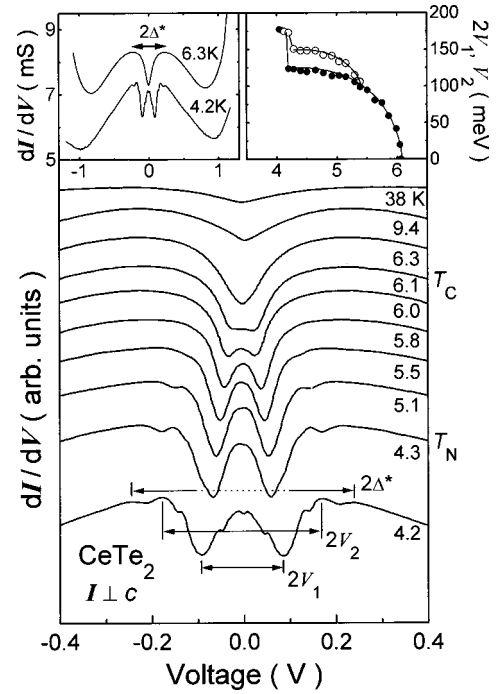


FIG. 2. Temperature variations of dI/dV for $I \perp c$ in a single-crystal CeTe_2 with increasing temperature from 4.2 K (bottom) to 38 K (top). The spectra are shifted vertically for clarity. Right inset represents the temperature dependence of the bias separation $2V_1$ (●) and V_2 (○) determined from the analysis of dI/dV data (see text). Left inset shows the dI/dV curves at temperatures 4.2 and 6.3 K in the overall bias range.

talline samples of LaTe_2 and CeTe_2 at various temperatures. The gap features are reproducible for several samples and different junctions with various resistance values over a wide range, 30–5000 Ω , which is much larger than the estimated sample resistance 0.1–1 Ω . In the top frame, the typical dI/dV curve for LaTe_2 at 60 K exhibits well-defined symmetric peaks at $V = \pm 0.85 \text{ V}$ with respect to the zero bias. The gap width of 1.70 eV is unchanged at least over the measured temperatures up to 120 K. In the middle frame, the curve 2 exhibits double-gap structures with the bias separations of 1.70 and 0.86 V. Here it is noteworthy that the former is twice the latter. This double structure may come from two junctions coexisting at the broken interface, as mentioned above; the former corresponds to $4\Delta/e$ of SIS (S is the semiconducting state with CDW, I is the insulating barrier) junction and the latter corresponds to $2\Delta/e$ of SIN (N is the normal state without CDW) junction, where Δ is half the energy gap. It is likely that the SIS junction is formed at a cleaved surface between layers in a grain, whereas the SIN junction is formed at a grain boundary. Also in CeTe_2 two gap values are observed, $4\Delta = 2.4 \text{ eV}$ in the curve 4 and $2\Delta = 1.2 \text{ eV}$ in the curve 3, respectively. Because the gap value is comparable to that for LaTe_2 , we attribute this gap to the CDW gap in CeTe_2 . If the empirical relation $2\Delta/k_B T_{\text{CDW}} = 12 - 14$ is used, then $2\Delta \sim 1 \text{ eV}$ yields $T_{\text{CDW}} \approx 1000 \text{ K}$. Therefore, no change of the gap value against temperatures up to 120 K is reasonable. However, there is a significant difference in the gap structure between

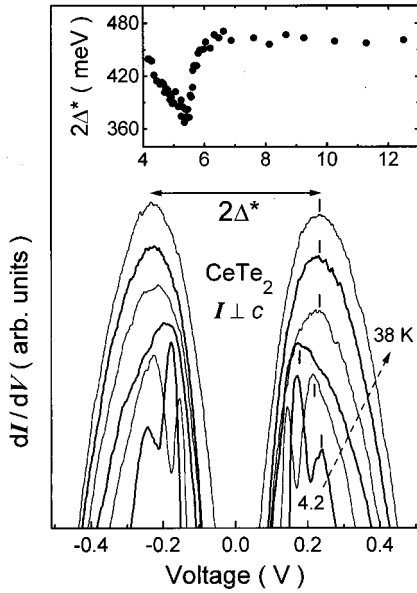


FIG. 3. Temperature variations of dI/dV for $I \perp c$ in a single crystal CeTe_2 at different temperatures 4.2, 4.3, 5.5, 6.3, 9.4, and 38 K from bottom to top. The temperature dependence of $2\Delta^*$ is displayed in the inset.

the two compounds. In contrast to the U-shaped spectra for LaTe_2 , the spectra of CeTe_2 is V shaped with electronic density-of-states within the gap. This in-gap state may originate from the hybridization of Ce $4f$ states with conduction-electron states. We will discuss this point later by the comparison with the data of optical conductivity.

At 4.2 K just below $T_N=4.3$ K, the dI/dV curve of CeTe_2 reveals subgap anomalies at $V_1=\pm 0.1$ V and $V_2=\pm 0.2$ V, which are indicated by arrows in the bottom frame of Fig. 1. Since the anomalies are reproducible for various junctions, they appear to be inherent. The subgap anomalies in the curve 6 disappear upon heating to 10 K above T_N to become the curve 5, whereas the main gap structure at $V=\pm 0.45$ V is unchanged. This disappearance should be only due to the thermal effect, because the junction is very stable and the main gap is reproduced. These two subgap anomalies found for polycrystalline samples are more clearly observed in single crystals, which is shown in Fig. 2. The bias separations are, respectively, denoted by $2V_1$ and $2V_2$. On heating, both V_1 and V_2 decrease suddenly at $T_N=4.3$ K and gradually decrease to vanish at $T_C=6.1$ K (see the right inset of Fig. 2). This temperature dependence is similar to that of the order parameter of a second-order phase transition. However, it is rather surprising that excitations of 0.1–0.2 eV (1000–2000 K) disappear only at 6.1 K. We have further examined the magnetic-field dependence of the subgap anomalies, which will be presented later.

The maximum at $V=\pm 0.24$ V ($2\Delta^*=0.48$ eV) was observed only in single crystals CeTe_2 for the bulk tunneling current in the c plane. The maximum possesses the strength of 40% of the background conductance, as seen in the left inset of Fig. 2. In order to trace the temperature dependence of $2\Delta^*$, the spectra are enlarged in Fig. 3. As the temperature is raised from $T_N=4.3$ K, $2\Delta^*$ initially decreases and turns to increases, then saturates to a value of 0.47 eV above

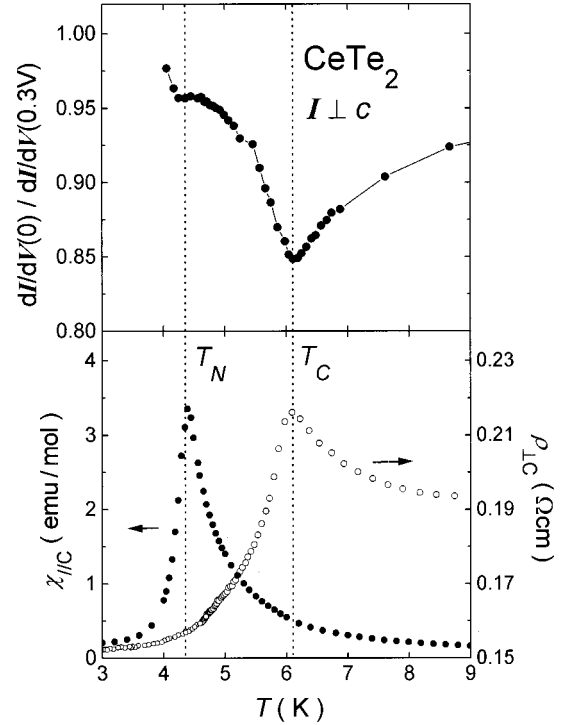


FIG. 4. Comparison of temperature dependence between the normalized zero-bias conductance $[dI/dV(0)]/[dI/dV(0.3\text{V})]$, the magnetic susceptibility χ for $B \parallel c$, and the electrical resistivity ρ for $I \perp c$.

$T_C=6.1$ K. For $T \geq T_C$, no temperature dependence in $2\Delta^*$ was observed as in 2Δ , but the magnitude of $2\Delta^*=0.47$ eV is nearly half of $2\Delta=0.9$ eV. The different values might be related to the shift in stoichiometry of the junctions and/or anisotropic nature of the gap in CeTe_2 . However, the well-reproducible observations of $2\Delta^*$ for $I \perp c$ in several single crystals allow us to exclude the sample dependence. The large gap 2Δ is then assumed to be the gap formed along the c axis, while the small one $2\Delta^*$ is in the c plane. This interpretation is based on the large anisotropy in the resistivity, $\rho(I \parallel c)/\rho(I \perp c) \sim 100$.¹⁴ Actually, we confirmed by optical microscopic observation that polycrystalline samples were cleaved preferably between layers perpendicular to the c axis, while thin-plate single-crystalline samples were cracked parallel to the c axis. Therefore, $2\Delta^*$ may be ascribed to the CDW gap in the c plane. This conjecture is strengthened by the fact that the value of $2\Delta^*$ is close to the gap value of 0.5 eV for CDW's in the Te layers of SmTe_3 .¹⁰ The strong variations of $2\Delta^*(T)$ below T_C indicate the significant effect of the magnetic ordering on the energy gap in the c plane. The minimum in $2\Delta^*(T)$ between T_N and T_C is probably associated with the competition between the three-dimensional antiferromagnetic order and the two-dimensional ferromagnetic order. The following rapid increase up to T_C can be a result of the loss of ferromagnetic order, which should be in favor of the CDW states.

Another remarkable feature of the dI/dV curves in Fig. 2 is the hump at zero bias, which fades out above T_C . For such a zero-bias hump, two possible origins are recorded: (i) magnetic scattering across the tunneling barrier by the interaction

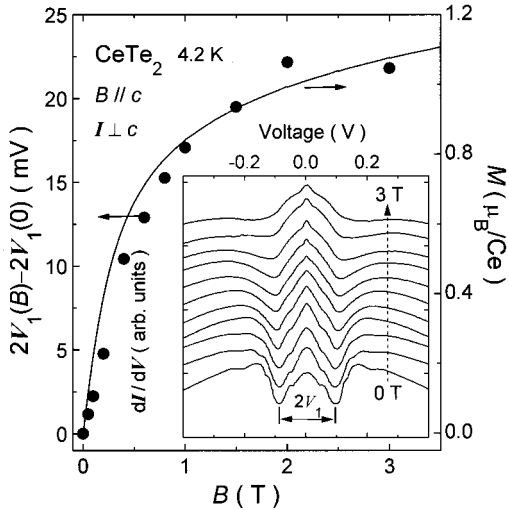


FIG. 5. Inset: magnetic-field variations of dI/dV spectra for a single crystal CeTe_2 taken in fields $B\parallel c$ at 0, 0.05, 0.1, 0.2, 0.4, 0.6, 0.8, 1.5, and 3 T from bottom to top. Magnetic-field dependence of the subgap $V_1(B\parallel c)$ at 4.2 K is well scaled with the magnetization curve $M(B\parallel c)$.

of the carrier spins with the localized $4f$ moments, the so-called Kondo scattering,^{2,22} and (ii) Andreev-like reflection at the metallic contact accidentally formed at the interface.^{23,24} In any case, the zero-bias feature should be a consequence of the magnetic transition because it disappears on heating exactly at $T_C = 6.1$ K. The normalized zero-bias conductance $[dI/dV(0)]/[dI/dV(0.3\text{ V})]$ also changes dramatically at both 4.3 and 6.1 K, as shown in Fig. 4. The former coincides with T_N determined as the peak in the magnetic susceptibility, and the latter agrees with T_C determined as the peak of the electrical resistivity.¹⁴ Therefore, the tunneling conductance indeed probes the electronic density-of-states affected by the magnetic transitions.

We further studied the magnetic-field dependence of the subgaps at 4.2 K in fields up to 3 T applied parallel to the c axis, the easy magnetization direction, using the same junction that was used for the temperature variation measurements in Fig. 2. The spectra in the inset of Fig. 5 show that the depth of the dips at $V_1 = \pm 0.1$ V decreases but the separation $2V_1$ increases as the magnetic field is increased. In Fig. 5, we plot the magnetic-field dependence of $2V_1(B) - 2V_1(0)$ together with the magnetization curve $M(B\parallel c)$ measured at 5 K. The nonlinear increase of $2V_1(B) - 2V_1(0)$ is well scaled with $M(B)$. This fact indicates that the magnetic order of CeTe_2 gives rise to the subgap anomalies through the spin polarization of electronic states by the internal magnetic field. The spectra in Fig. 5 also show that the background conductance is raised with magnetic field. This change may be related to the field alignment of the Ce magnetic moments in parallel on both barrier sides. The increase of conduction driven by the alignment of magnetic moments is analogous to the field-induced spin-polarized tunneling in layered manganites $(\text{La, Sr})_3\text{Mn}_2\text{O}_7$.²⁵

Finally, we point out the close relation between the present tunneling spectra dI/dV and optical-conductivity spectra σ_{opt} obtained by optical-reflection measurements.²⁶

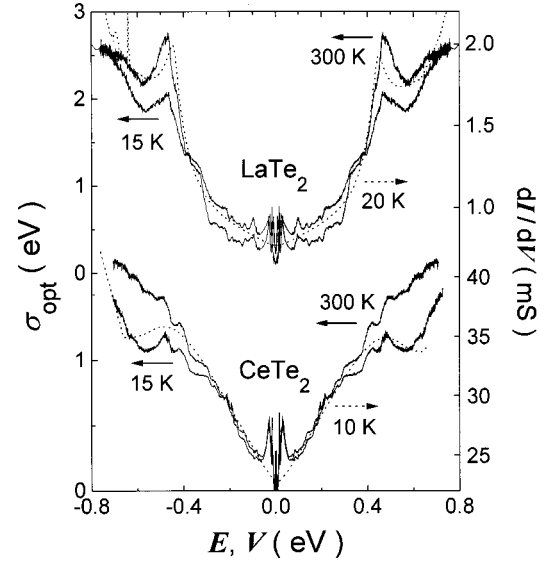


FIG. 6. Comparison of the tunneling conductance dI/dV (dashed line) with the optical conductivity σ_{opt} (full line) for polycrystalline samples of LaTe_2 and CeTe_2 , respectively. The data of σ_{opt} are taken from Ref. 26.

In Fig. 6, the data of dI/dV for polycrystalline samples of LaTe_2 and CeTe_2 are, respectively, compared with symmetrized data of $\sigma_{\text{opt}}(E)$. It is remarkable that the overall spectral features of dI/dV coincide with those of σ_{opt} . Namely, σ_{opt} for LaTe_2 is nearly flat in a low-energy region below 0.3 eV and then increases rapidly with increasing photon energy, whereas σ_{opt} for CeTe_2 is V shaped. This quantitative agreement between the tunneling and optical spectra suggests that 2Δ in dI/dV and the energy gap E_g in σ_{opt} have the same origin. The main structure in σ_{opt} is observed at 0.5 eV for both LaTe_2 and CeTe_2 which is essentially independent of temperature up to 300 K. If the structures in σ_{opt} reflect the direct transition across the band gap from the valence band to the conduction band, E_g should equal to 2Δ . However, we find the relation $\Delta \approx E_g$ for both compounds. The reason of this twofold discrepancy is not clear at present, and we conjecture that the optical measurement does not probe the quasiparticle excitations, instead it sees the direct band gap of the conduction electrons. Further studies on the anisotropic gap structures are necessary by optical-reflection measurements on single-crystalline samples, together with photoemission spectroscopic measurements that probe the quasiparticle density of states.

In conclusion, the energy gap of $2\Delta = 0.9$ and 1.2 eV was observed for the layered compounds LaTe_2 and CeTe_2 respectively. Since the main gap 2Δ in CeTe_2 is comparable to the CDW gap in LaTe_2 the gap in CeTe_2 is also ascribed to the CDW gap. The tunneling spectra of both systems, respectively, correspond well with the optical conductivity spectra. A smaller gap $2\Delta^* = 0.5$ eV was found for the bulk tunneling current in the c plane of single crystals of CeTe_2 . The important observation is that $2\Delta^*$ decreases when the Ce magnetic moments order ferromagnetically below T_C . This fact and the remarkable change in the zero-bias conductance at both T_C and T_N point to the significant interplay of the CDW's and the magnetic orders in CeTe_2 .

- *Present address: NHMFL, Pulse Field Facility, LANL, Los Alamos, NM 87545.
- ¹For example, see *Electronic Properties of Inorganic Quasi One-Dimensional Compounds*, edited by P. Monceau (Reidel, Dordrecht, 1985); *Charge Density Wave in Solids*, edited by L. Gor'kov and G. Grüner (North-Holland, Amsterdam, 1989); G. Grüner, *Density Waves in Solids* (Addison-Wesley, Longmans, Massachusetts, 1994).
- ²E. L. Wolf, *Principles of Electron Tunneling Spectroscopy* (Oxford, New York, 1985).
- ³R. Sooryakumar and M. V. Klein, Phys. Rev. Lett. **45**, 660 (1980).
- ⁴F. Galli, S. Ramakrishnan, T. Taniguchi, G. J. Nieuwenhuys, J. S. Mydosh, S. Geupel, J. Lüdecke, and S. van Smaalen, Phys. Rev. Lett. **85**, 158 (2000).
- ⁵M. H. Whangbo, D. K. Seo, and E. Canadell, in *Physics and Chemistry of Low-Dimensional Inorganic Conductors*, edited by C. Schlenker, M. Greenblatt, J. Dumas, and S. V. Smaalen (Plenum, New York, 1996).
- ⁶M. Grupe and W. Urland, J. Less-Common Met. **170**, 271 (1991).
- ⁷B. Foran, S. Lee, and M. C. Aronson, Chem. Mater. **5**, 974 (1993).
- ⁸E. DiMasi, M. C. Aronson, B. Foran, and S. Lee, Physica B **206&207**, 386 (1995).
- ⁹E. DiMasi, M. C. Aronson, J. F. Mansfield, B. Foran, and S. Lee, Phys. Rev. B **52**, 14 516 (1995).
- ¹⁰G.-H. Gweon, J. D. Denlinger, J. A. Clack, J. W. Allen, C. G. Olson, E. DiMasi, M. C. Aronson, B. Foran, and S. Lee, Phys. Rev. Lett. **81**, 886 (1998).
- ¹¹R. Wang, H. Steinfink, and W. F. Bradley, Inorg. Chem. **5**, 142 (1966).
- ¹²E. DiMasi, B. Foran, M. C. Aronson, and S. Lee, Phys. Rev. B **54**, 13 589 (1996).
- ¹³A. Kikuchi, J. Phys. Soc. Jpn. **67**, 1308 (1999).
- ¹⁴M. H. Jung, B. H. Min, Y. S. Kwon, I. Oguro, F. Iga, T. Fujita, T. Ekino, T. Kasuya, and T. Takabatake, J. Phys. Soc. Jpn. **69**, 937 (2000).
- ¹⁵S. M. Park, S. J. Park, and S. J. Kim, J. Solid State Chem. **140**, 300 (1998).
- ¹⁶K. Stöwe, J. Solid State Chem. **149**, 155 (2000).
- ¹⁷M. H. Jung, Y. S. Kwon, and T. Suzuki, Physica B **240**, 83 (1997).
- ¹⁸M. H. Jung, K. Umeo, T. Fujita, and T. Takabatake, Phys. Rev. B **62**, 11 609 (2000).
- ¹⁹J. G. Park, I. P. Swainso, W. J. L. Buyers, M. H. Jung, and Y. S. Kwon, Physica B **241-243**, 684 (1998).
- ²⁰J. G. Park, Y. S. Kwon, W. Kockelmann, M. J. Bull, I. P. Swainson, K. A. McEwen, and W. J. L. Buyers, Physica B **281&282**, 451 (2000).
- ²¹T. Ekino, T. Takabatake, H. Tanaka, and H. Fujii, Phys. Rev. Lett. **75**, 4262 (1995).
- ²²J. Klug, A. Nowack, and W. Jeitschko, Fiz. Nizk. Temp. **18**, 761 (1992) [Sov. J. Low Temp. Phys. **18**, 539 (1992)].
- ²³A. A. Sinchenko, Yu. I. Latyshev, S. G. Zybtshev, I. G. Gorlova, and P. Monceau, Phys. Rev. B **60**, 4624 (1999).
- ²⁴F. Laube, G. Goll, H. v. Löhneysen, M. Fogelström, and F. Lichtenberg, Phys. Rev. Lett. **84**, 1595 (2000).
- ²⁵T. G. Perring, G. Aeppli, T. Kimura, Y. Tokura, and M. A. Adams, Phys. Rev. B **58**, 14 693 (1998).
- ²⁶M. H. Jung, Y. S. Kwon, T. Kinoshita, and S. Kimura, Physica B **230-232**, 151 (1997).